

Dual-Isotope SPECT of Skull-Base Invasion of Head and Neck Tumors

Mitsutaka Fukumoto, Shoji Yoshida, Daisuke Yoshida and Seiji Kishimoto

Departments of Radiology and Otolaryngology, Kochi Medical School, Kochi, Japan

Skull-base invasions of head and neck tumors were examined by simultaneous bone and tumor dual-isotope SPECT (S-SPECT) with ^{99m}Tc -hydroxy-methylene-diphosphonate (^{99m}Tc -HMDP) and ^{201}Tl -chloride. The effectiveness and reliability of tumor diagnosis by this method was the primary interest in this study. **Methods:** Before S-SPECT imaging, a phantom experiment using dried skull-bone specimens was performed to establish anatomical details of the skull base with the SPECT camera. Radionuclide crosstalk, window widths and control patients were also examined prior to S-SPECT imaging. Twenty patients with suspected tumor invasion of the skull base underwent S-SPECT. **Results:** Preliminary experiments revealed that crosstalk effects could be disregarded with adequate window width and routine administrative doses of the radionuclides. S-SPECT detected bone destruction and the extent of tumor invasion for all 12 patients in whom skull-base involvement was diagnosed by CT or MRI. For the three patients in whom CT or MRI revealed no tumor invasion, the S-SPECT images did not show any abnormal accumulation in similar regions. In the remaining five patients without CT and MRI confirmation of skull-base invasion, the S-SPECT findings showed skull-base abnormalities in three. Tumor invasion was confirmed surgically or by clinical follow-up. The remaining two patients had negative S-SPECT images. **Conclusion:** S-SPECT is an effective and reliable diagnostic technique for detecting tumor invasion in the complex bony regions of the skull base.

Key Words: single-photon emission computed tomography; technetium-99m-HMDP; thallium-201-chloride; skull base invasion; head and neck tumors

J Nucl Med 1995; 36:1740-1746

Malignant head and neck tumors are commonly known to invade the skull base. Although not all invasive patterns are direct, occasionally there is protrusion through the neurovascular foramina. In many cases, resorption or destruction of the surrounding bony regions is observed. To date, the diagnosis of lesions in the skull base have been limited to the use of CT and MRI. When the lesion is localized near the cortical regions of the skull-base bone,

however, detection by CT or MRI is often inconclusive. CT images are sometimes obscured by artifacts, arising from complex bony structures of the skull base, whereas MRI has the inherent drawback of weak signal detection (signal void) from the bone cortex.

Several studies have shown that planar bone scintigraphy is a useful technique for demonstrating skull bone invasion of head and neck tumors (1-5), but the specific localization of these lesions was often difficult to ascertain because of the complexity of the skull base. Brown et al. (6) reported that the normal and abnormal transaxial anatomy of the face and skull could be clearly defined by SPECT. Despite their significant results, at the time, SPECT had poor spatial resolution. This problem has been greatly reduced with the introduction of three-detector SPECT cameras equipped with fanbeam collimators. This instrumentation provides significantly better spatial resolution and image clarity than previous SPECT models.

Bone SPECT with ^{99m}Tc -HMDP has become an important diagnostic tool. Yui et al. (7) showed how bone SPECT can be successfully used in skull-base regions and has high sensitivity for bone lesions detection. Moreover, the sensitivity of this method can provide earlier diagnosis of bone abnormalities. These findings are often more conclusive than those obtained by CT, MRI or planar bone scintigraphy.

In addition, ^{201}Tl -Cl, a radionuclide that displays preferential accumulation in a variety of tumor types, is commonly used in SPECT tumor imaging. Several reports have demonstrated its efficacy in evaluating and localizing malignant tissue, especially in the lungs (8,11), brain (9,10) and skull base (12,13).

This study was undertaken to provide a reliable diagnostic method for the early detection of skull-base invasion of head and neck tumors. To achieve our goal, we used simultaneous bone and tumor dual SPECT (S-SPECT) imaging for co-localization of bone and tumor-specific radionuclides in patients with suspected skull-base invasion.

MATERIALS AND METHODS

Preliminary Study

Prior to clinical application, a preliminary examination of a dried skull was conducted to establish anatomical details of the skull base. A dried skull was first labeled by immersion for 1 hr in 4000 ml ^{99m}Tc -HMDP diluted with physiological saline and sub-

Received Sept. 13, 1994; revision accepted Jan. 26, 1995.
For correspondence or reprints contact: Mitsutaka Fukumoto, MD, Department of Radiology, Kochi Medical School, Kohasu, Okoh-cho, Nankoku-City, Kochi 783, Japan.

sequently dried with warm air to produce a phantom specimen. Bone SPECT was performed on the phantom skull and a control image of the skull base was obtained. The phantom image was compared with a bone SPECT image of the skull of a normal patient who had no symptoms of head and neck disease. Additionally, the neurovascular foramina of the ^{99m}Tc -HMDP labeled dry skull were filled with small cotton balls soaked with $^{201}\text{TlCl}$ (containing approximately 10–25 MBq each), and S-SPECT was performed to determine the anatomical locations of the foramina by superimposing them on the bone SPECT image.

Crosstalk evaluation of the radionuclides was examined in the range of 68–80 keV to determine ^{99m}Tc scatter effects on the ^{201}Tl photopeak. The count per unit volume of ^{201}Tl measured from a homogeneous ^{201}Tl aqueous solution (37.5 MBq/1 ml) was designated as variable A. In addition, a mixed aqueous solution containing equal volumes of ^{201}Tl (37.5 MBq/1 ml mixed solution) and ^{99m}Tc (37.5 MBq/1 ml mixed solution) was examined. In this case, the count per unit volume of ^{201}Tl of the above mixture was variable B. The crosstalk (CR) effect that ^{99m}Tc had on the ^{201}Tl window was approximated by the following formula:

$$\text{CR} = (\text{B} - \text{A})/\text{A} \times 100 (\%).$$

The energy window width for S-SPECT was changed to 10%, 15%, 20% and 30% and the respective crosstalks were calculated.

Because administered doses of radionuclides are different in clinical practice, ^{99m}Tc crosstalk in the energy window of ^{201}Tl (at 10% window width) was also studied with a variety of mixed solutions. The radionuclides were combined in aqueous solutions with the proportions of ^{99m}Tc to ^{201}Tl ranging from 4:1 to 4:4 and subsequently examined for crosstalk. We chose these mixture ratios based on the results from single-isotope SPECT analysis of normal physiological distribution ratios of ^{99m}Tc -HMDP (555 MBq, 4.5 hr) and $^{201}\text{TlCl}$ (111 MBq, 2.0 hr) obtained from the skull bases of normal individuals. Normal physiological distribution ratios in the range of 4:2 to 4:3 were observed in the preliminary clinical trials and were used for reference in the clinical studies.

Clinical Study

Following the preliminary studies, 20 patients (16 men, 4 women, aged 22 to 78 yr) with suspected skull-base tumor invasion had S-SPECT. The imaging protocol was:

1. Intravenous injection of ^{99m}Tc -HMDP (555 MBq) with a 2.5 hr waiting time.
2. Whole-body planar bone scintigraphy was performed.
3. After bone scintigraphy, intravenous injection of $^{201}\text{TlCl}$ (111 MBq).
4. At 2 hr postinjection of $^{201}\text{TlCl}$ (4.5 hr postinjection of ^{99m}Tc -HMDP), S-SPECT of the skull base was performed.
5. Bone and tumor S-SPECT images were evaluated.

A three-detector SPECT camera equipped with a fanbeam collimator with 7.3 mm spatial resolution (FWHM, at the rotation center) was used for the preliminary and clinical studies.

Each detector was rotated at 4° step angles (30-sec step intervals). Fanbeam projection data from 90 steps were acquired over 15 min and collected on a 256 × 256 matrix. The fanbeam projection data were then converted to the parallel-beam projection data on a 128 × 128 matrix, and SPECT images with 1.7 mm slice thickness were constructed by Butterworth and ramp filters for preprocessing and backprojection, respectively. Axial, coronal and sagittal images of bone and tumor SPECT were obtained simultaneously. Diagnosis of the skull-base invasion was made by

TABLE 1
S-SPECT Results of Skull-Base Invasion

Bone SPECT	Tumor SPECT	Diagnosis
Positive	Positive	Tumor contacting the skull base.
Positive	Negative	Skull base bone abnormality with no tumor invasion. Possibility of no ^{201}Tl uptake (false negative) or bony inflammation around tumor.
Negative	Positive	Pattern is rare. Protrusion of tumor through the neurovascular foramina with no invasion.
Negative	Negative	Skull base is not involved. No tumor contact with the skull base.

analysis of both kinds of images. Examples of positive or negative findings and a brief description of their significance are given for each radionuclide in Table 1.

RESULTS

Preliminary Study

Comparison of bone SPECT images obtained from the dried skull phantom and the normal control patient revealed no major differences in skull-base anatomical details (Fig. 1). Application of S-SPECT to the dry bone phantom (labeled with ^{99m}Tc -HMDP) containing $^{201}\text{TlCl}$ labeled cotton balls in the neurovascular foramina made it possible to determine the locations of the foramina in S-SPECT images (Fig. 2). Results of the crosstalk study, in equal doses of ^{99m}Tc and ^{201}Tl , revealed slightly increased crosstalk in the 10%–20% window width, whereas in the 30% window width, greater than 30% crosstalk was observed (Table 2). When the mixture ratios of ^{99m}Tc to ^{201}Tl were changed, the crosstalk was slightly increased, except when the mixture ratio of ^{99m}Tc to ^{201}Tl was 4:1 (Table 2).

Clinical Study

The results of S-SPECT evaluation of skull-base tumor invasion and other modalities (CT, MRI and surgical findings) are given in Table 3. For the patients with conclusive CT and MRI results of skull-base destruction and tumor invasion, S-SPECT also visualized abnormal tracer accumulations in both the bone and tumor SPECT images.

In the three patients in whom CT and MRI showed noncontacting tumor at the skull base, S-SPECT analysis revealed no alterations in the bony anatomy of the skull base and a complete separation of tumor from the bone. The remaining five patients displayed problematic signs of skull-base destruction. S-SPECT detected tumor invasion in three of five patients with inconclusive findings; surgery later confirmed tumor invasion. In two patients with suspected skull-base invasions, S-SPECT was negative and surgery confirmed the S-SPECT results. Four typical cases of S-SPECT application are illustrated (Figs. 3–6). Al-

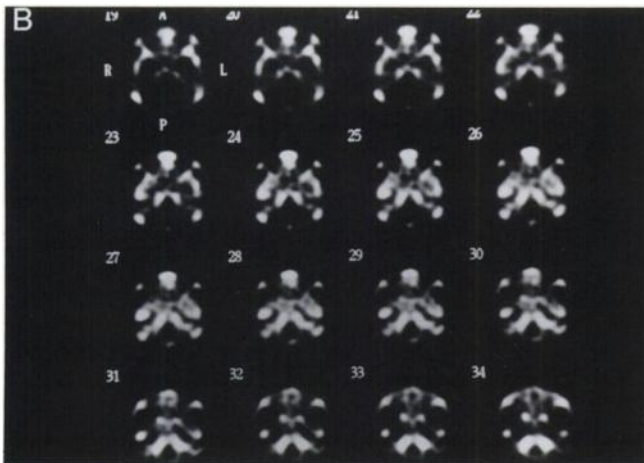
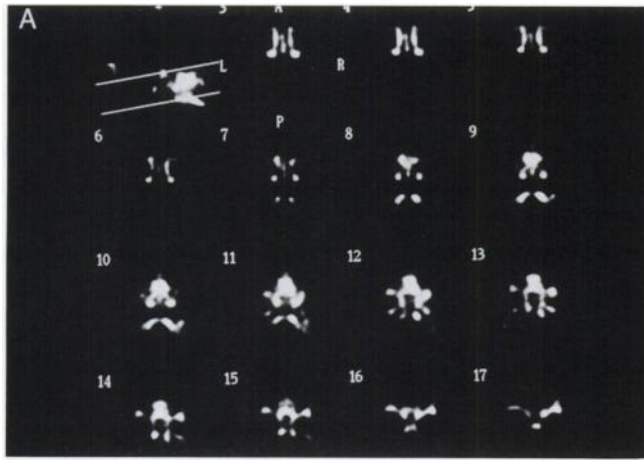


FIGURE 1. Bone SPECT images of skull-base regions from a ^{99m}Tc -HMDP-labeled dried skull (A) and control patient (B). Comparison of anatomical structures revealed no major differences. No mandible is present on the dried skull specimen.

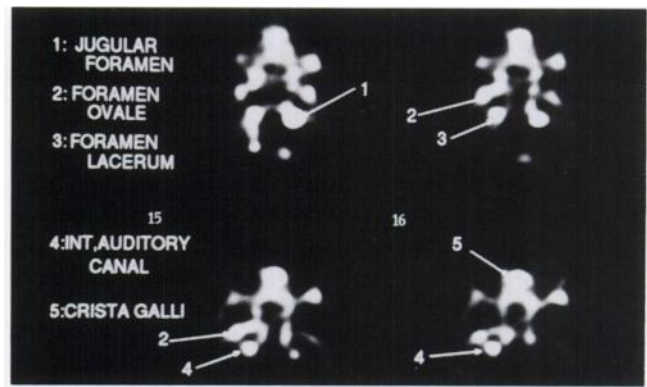


FIGURE 2. SPECT images of the ^{99m}Tc -HMDP-labeled dried skull containing small cotton swabs in the major neurovascular foramina. Cotton balls labeled with ^{201}Tl also were placed around the Crista galli.

TABLE 2
Crosstalk Study Results

Comparison of Window Width to Crosstalk (^{201}Tl window)	
Window width	Crosstalk ratio
30% width	37% \pm 2.5%
20% width	18% \pm 2.1%
15% width	11% \pm 2.2%
10% width	7% \pm 1.5%
Crosstalk Evaluation of Four Mixture Ratios (^{201}Tl window)	
Mixture ratio (^{99m}Tc : ^{201}Tl)	Crosstalk ratio (10% width fixed)
4:1	35% \pm 5.2%
4:2	20% \pm 4.1%
4:3	17% \pm 3.1%
4:4	11% \pm 2.7%

TABLE 3
Assessment of Skull Base Invasion

Patient no.	Diagnosis	CT/MRI	S-SPECT in Skull Base			Invasion (ope, biopsy)
			Bone SPECT	Tumor SPECT	Evaluation	
1	Maxillary ca SCC	Positive	Positive	Positive	Invasion	(+)
2	Maxillary ca SCC	Positive	Positive	Positive	Invasion	(+)
3	Parotid ca Adeno	Positive	Positive	Positive	Invasion	(+)
4	Nasal neuroblastoma	Obscure	Positive	Positive	Invasion	(+)
5	Nasal ca SCC	Positive	Positive	Positive	Invasion	(+)
6	Epipharyngeal ca SCC	Positive	Positive	Positive	Invasion	(+)
7	Epipharyngeal ca SCC	Positive	Positive	Positive	Invasion	(+)
8	Maxillary ca SCC	Positive	Positive	Positive	Invasion	(+)
9	Epipharyngeal ca SCC	Positive	Positive	Positive	Invasion	(+)
10	Epipharyngeal ca SCC	Obscure	Positive	Positive	Invasion	(+)
11	Chondrosarcoma. pre op	Positive	Positive	Positive	Invasion	(+)
12	Maxillary ca SCC	Negative	Negative	Negative	No Invasion	(-)
13	Maxillary lymphoma	Obscure	Positive	Negative	Invasion	(+)
14	Maxillary ca SCC	Negative	Negative	Negative	No Invasion	(-)
15	Chondrosarcoma. post op	Obscure	Positive	Negative	No Residual	(-)
16	Palate inverted papilloma	Positive	Positive	Negative	Invasion	(+)
17	Undifferentiated ca*	Positive	Positive	Negative	Invasion	(+)
18	Maxillary ca SCC	Negative	Negative	Negative	No Invasion	(-)
19	Epipharyngeal ca SCC	Positive	Positive	Positive	Invasion	(+)
20	Maxillary ca SCC	Obscure	Positive	Negative	No Invasion	(-)

*Metastatic tumor (parapharyngeal origin).

ca = carcinoma; adeno = adenocarcinoma; SCC = squamous-cell carcinoma.

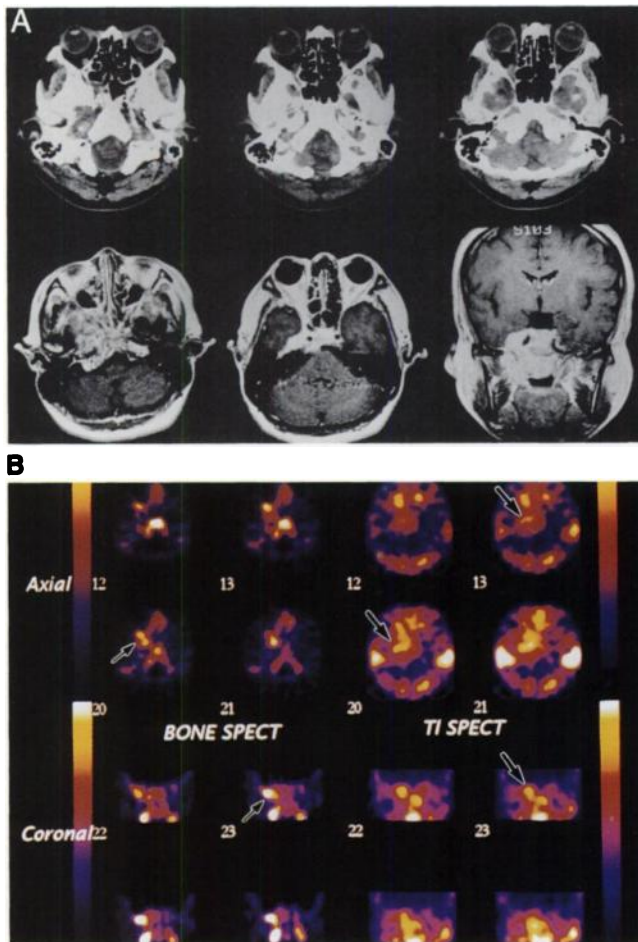


FIGURE 3. (A) CT (above) and MRI (below) of a 67-yr-old woman with epipharyngeal squamous-cell carcinoma reveal a conspicuous lesion on the right side indicative of skull-base invasion. (B) S-SPECT shows abnormal high ^{99m}Tc -HMDP accumulations (small arrows) corresponding to tumor-positive sites (large arrows) in a region just below the right foramen lacerum.

though the sample number was small, we performed statistical analysis. S-SPECT sensitivity for detecting skull-base tumor invasion was 93.3% (Table 4). S-SPECT bone image, on the other hand, had a sensitivity, specificity and accuracy of 100%, 60% and 90%, respectively (Table 4). The sensitivity, specificity and accuracy of tumor S-SPECT were 80%, 100% and 85%, respectively (Table 4). We found no accumulation of ^{201}Tl in patients with malignant lymphoma, undifferentiated carcinoma or inverted papilloma.

A postoperative case of chondrosarcoma at the skull base was of interest. Although the tumor was completely removed, CT scans showed abnormal soft-tissue density in the skull base as a result of bone reinforcement techniques and postoperative changes (Fig. 6A). In this patient, CT determination of residual abnormality or recurrent lesion was not possible. S-SPECT, however, showed that bone damage was a result of surgery, and tumor SPECT revealed the absence of malignant tissue (Fig. 6B).

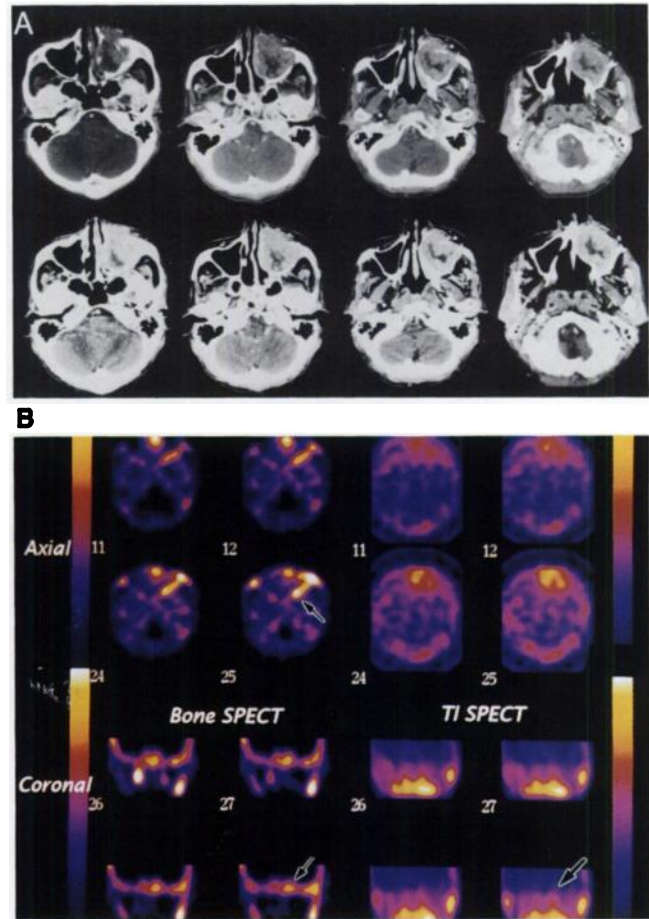


FIGURE 4. (A) CT scans (bone-window CT above, contrast-enhanced CT below) from a 66-yr-old man with maxillary cancer localized in the postero-lateral wall of the maxillary sinus are negative for skull-base invasion. (B) Bone SPECT revealed high accumulation in the skull base (small arrows); tumor SPECT was negative in this area (large arrow).

DISCUSSION

Skull-base invasion of head and neck tumors significantly affect a patient's prognosis. Therefore, it is extremely important to detect the location and determine the extent of tumor involvement in this region of the skull. Other clinicians (1-5) have reported that bone scintigraphy was sufficient for detecting head and neck tumor invasions at the skull bone. Unfortunately, the complex structure of the skull base and lack of distinction between the numerous structure in this region are major limitations of bone scintigraphy. Brown et al. (6) distinguished between normal and abnormal bony regions fairly distinctly by using bone SPECT, but their findings were limited by the spatial resolution of the SPECT camera. Technological improvements have revolutionized SPECT imaging, making it more accurate and reliable for detecting tracer localization.

In many patients, extensive tumor development and skull-base destruction can be diagnosed accurately with CT or MRI. Yui et al. (7,13) reported that bone SPECT could detect skull base abnormalities, even though CT or

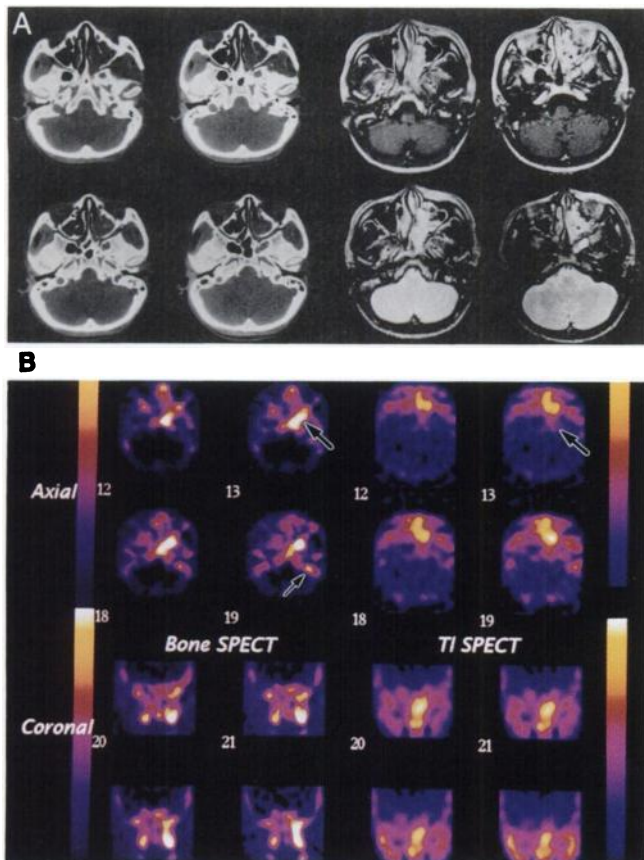


FIGURE 5. (A) CT and MRI scans from a 22-yr-old woman with nasal neuroblastoma were inconclusive for skull-base invasion. (B) S-SPECT revealed positive bone reactivity in the posterior nasal region with some tumor invasion (large arrows). A small accumulation of tracer was visualized in the right temporal bone in the bone SPECT image (small arrow).

MRI showed normal anatomy, when a tumor existed just below or near the skull base. Their studies, however, used single SPECT analysis of the radionuclide, and the relationships of bone with the tumor were inconclusive.

In our study, a direct comparison of tumor and bone could be obtained by simultaneous visualization of both radionuclides. Technetium-99m-HMDP is one of the most sensitive radiopharmaceuticals for detecting bone disease, and although false-positives are sometimes observed, confirmation can be achieved by examining the accumulation of $^{201}\text{Tl-Cl}$ relative to the false-positive site.

In this study, delayed $^{201}\text{Tl-Cl}$ images were suitable for detecting malignant tumors because of delayed washout observed in malignancies (8,15–17). Some studies using $^{201}\text{Tl-Cl}$ found that only the early image was used to obtain the tumor SPECT image and that a delayed image was not acquired (12,18–21). This protocol is possible if positive determination of the tumor as malignant can be made by biopsy or other methods.

When reactive inflammation has an effect on the skull-base regions, $^{201}\text{Tl-Cl}$ may show high accumulations in the inflamed areas in early images. In this situation, it is often difficult to determine whether these results reflect actual

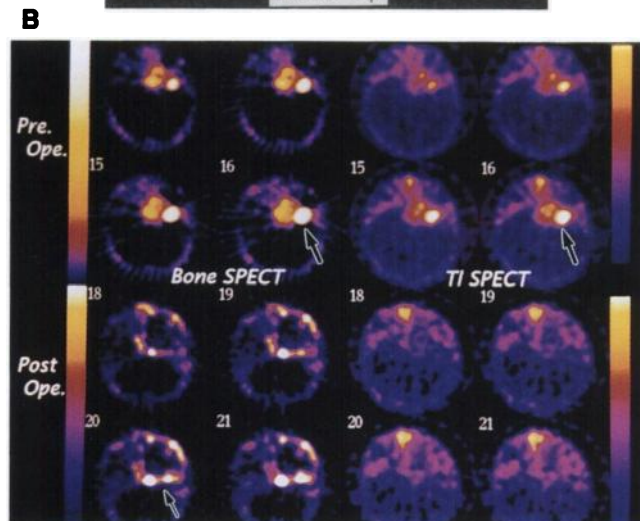
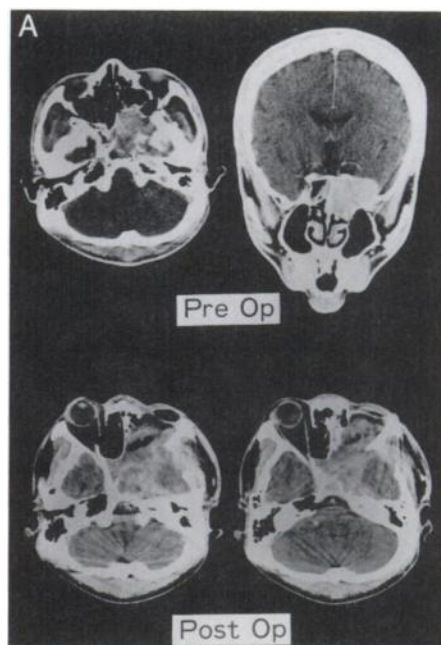


FIGURE 6. (A) Preoperative CT scan from a 37-yr-old man with chondrosarcoma of the skull base clearly revealed skull-base involvement. (B) Preoperative S-SPECT images were positive. The skull base was extensively invaded (large arrows) with destruction of bony regions. Postoperative S-SPECT revealed a positive bone SPECT as a result of reconstructive measures in the skull base (small arrow) and complete absence of ^{201}Tl accumulation in the tumor SPECT, indicating complete removal of malignant tissue.

invasion and changes in bone structure or an inflammatory response. False-positive results can be avoided by analyzing the delayed images. Thallium-201 Cl accumulations in inflammatory disease or benign lesions have been shown to decrease gradually with time, whereas delayed washout was observed in malignant tumors (8,22). Examination of the delayed image is an accurate method because it allows better differentiation between inflammatory and benign lesions from malignant lesions. In our study, we waited 2 hr before imaging, which appeared to be a suitable amount of time to permit contrast of the tumor from the surrounding tissues.

TABLE 4
Sensitivity, Specificity and Accuracy of Bone
and Tumor SPECT

	Sensitivity	Specificity	Accuracy
Bone SPECT	100%	60%	90%
Tumor SPECT	80%	100%	85%

S-SPECT detectability of skull base invasion = 93.3%.

A drawback of tumor SPECT using ^{201}Tl -Cl is no significant accumulation of ^{201}Tl -Cl in certain tumors in some patients. Yui et al. (23) also reported an absence of labeling in the first two types of manifestations. On the other hand, Sehweil et al. (24) reported that detectability of mediastinal lymphoma using ^{201}Tl was 84.6%. They reported negative scans for patients with Hodgkin's and non-Hodgkin's lymphoma. Nonaccumulation of ^{201}Tl is not a rare phenomenon in some types of malignant tumor. Further examination with regards to cellular kinetics of each tumor type is required.

Tumors of squamous-cell variety, however, were detected in this study with high specificity and sensitivity, indicating the usefulness of ^{201}Tl -Cl for reliable detection of these types of tumors. Most malignant head and neck tumors are classified as squamous-cell carcinoma, which is the basis for using S-SPECT in head and neck tumors. When we evaluate negative ^{201}Tl uptake SPECT images of tumors, we must determine whether there was ^{201}Tl accumulation in the tumor to avoid false-negative results. Thallium is believed to act as a potassium analog that can stimulate the activity of the Na^+ - K^+ ATP-ase dependent pump of cell membranes, resulting in active transport of ^{201}Tl into the cytoplasm. Although thallium uptake is not identical to potassium (i.e., ^{201}Tl appears to bind to two sites on the enzyme), this process is also sensitive to ouabain and sodium fluoride, which block the Na^+ - K^+ pump (25). Delayed washout (or possibly prolonged uptake) in metastatic tissue may be reflective of the Na^+ - K^+ -ATP-ase activities of the tissue's constituent cells, a difference that may explain the variation in thallium accumulation in different tumors (17,26).

The results of S-SPECT for detecting skull-base invasion were 93.3%. It must be emphasized that the combination of bone and tumor SPECT imaging enabled considerably higher detectability rates than either modality alone. Furthermore, if tumor detection by CT or MRI is possible, it can augment S-SPECT to evaluate the extent of bone involvement and localized reactive inflammation. For example, S-SPECT imaging may indicate an abnormality in a wider region of the skull base than CT or MRI. On the other hand, S-SPECT imaging proved useful in localizing skull-base invasions undetectable by both CT and MRI; tumor invasion was later confirmed by surgery and appeared to be silent or subclinical in nature.

CONCLUSION

S-SPECT is a useful technique that provides a complete anatomical and physiological picture, detailing normal and abnormal tissues. Even when skull-base destruction was evident on CT or MRI, S-SPECT clearly visualized the lesion as well as changes in the bone that were undetectable morphologically by CT or MRI. S-SPECT also proved an extremely useful diagnostic tool for the detection of silent or subclinical lesions and possible recurrent malignancies in instances when the CT or MRI results were inconclusive.

ACKNOWLEDGMENTS

The authors thank Mr. Naoki Akagi, Kochi Medical School, for assistance with the SPECT camera and Mr. Patrick Nahirney for reviewing and preparing the manuscript.

REFERENCES

- Alexander JM. Radionuclide bone scanning in the diagnosis of lesions of the maxillofacial region. *J Oral Surg* 1976;34:249-256.
- Higashi T, Sugimoto K, Shimura A, et al. Technetium-99m bone imaging in the evaluation of cancer of the maxillofacial region. *J Oral Surg* 1979;37:254-259.
- Bergstedt HF, Linf MG. Facial bone scintigraphy. *Act Rad Diag* 1981;22:609-618.
- Baker HL, Woodbury DH, Krause CJ, et al. Evaluation of bone scan by scintigraphy to detect subclinical invasion of the mandible by squamous cell carcinoma of the oral cavity. *Otolaryngol Head Neck Surg* 1983;90:327-336.
- Gates GF, Goris ML. Maxillary-facial abnormalities assessed by bone imaging. *Radiology* 1976;121:677-682.
- Brown ML, Keyes JW, Leonard PF, et al. Facial bone scanning by emission tomography. *J Nucl Med* 1978;18:1184-1188.
- Yui N, Togawa T, Kinoshita F, et al. Assessment of skull base involvement of nasopharyngeal carcinoma by bone SPECT using three detector system. *Kaku Igaku* 1992;29:37-47.
- Tonami N, Shuke N, Yokoyama K, et al. Thallium-201 single-photon emission computed tomography in the evaluation of suspected lung cancer. *J Nucl Med* 1989;30:997-1004.
- Black KL, Hawkins RA, Kim KT, Becker DP, Lerner C, Marciano D. Use of thallium-201 SPECT to quantitate malignancy grade of glioma. *J Neurosurg* 1989;71:342-346.
- Kim KT, Black KL, Marciano D, et al. Thallium-201 SPECT imaging of brain tumors: methods and results. *J Nucl Med* 1990;31:965-969.
- Matsuno S, Tanabe M, Kawasaki Y, et al. Effectiveness of planar image and single-photon emission computed tomography of thallium-201 compared with gallium-67 in patients with primary lung cancer. *Eur J Nucl Med* 1992;19:86-95.
- Togawa T, Yui N, Kinoshita F, Shimada F, Omura K, Takemiya S. Visualization of nasopharyngeal carcinoma with Tl-201 chloride and a three-head rotating gamma camera SPECT system. *Ann Nucl Med* 1993;7:105-113.
- Yui N, Sekiya N, Akiyama Y, et al. Single-photon emission computed tomography in the diagnosis of skull base invasion of nasopharyngeal carcinoma. *Kaku Igaku* 1986;23:367-373.
- Yui N, Kinoshita F, Akiyama Y, et al. Clinical evaluation of transaxial bone imaging with technetium-99m-phosphate compounds. *Radioisotopes* 1982;31:515-528.
- Jinnouchi S, Hoshi H, Ohnishi T, et al. Thallium-201 SPECT for predicting histological types of meningiomas. *J Nucl Med* 1993;34:2091-2094.
- Mahmoud El-Desouki. Thallium-201 thyroid imaging in differentiating benign from malignant thyroid nodules. *Clin Nucl Med* 1991;16:425-430.
- Ochi H, Sawa H, Fukuda T, et al. Thallium-201-chloride thyroid scintigraphy to evaluate benign and/or malignant nodules: usefulness of the delayed scan. *Cancer* 1982;50:236-240.
- Kaplan WD, Takvorian T, Morris JH, Rumbaugh CL, Connolly BT, Atkins HL. Thallium-201 brain tumor imaging: a comparative study with pathologic correlation. *J Nucl Med* 1987;28:47-52.
- Schwartz RB, Carvalho PA, Alexander E, Loeffler JS, Folkert R, Holman BL. Radiation necrosis versus high-grade recurrent glioma: differentiation

- by using dual isotope SPECT with ^{201}Tl and $^{99\text{m}}\text{Tc}$ -HMPAO. *Am J Neuro-radiol* 1991;12:1187-1192.
20. Ancrì D, Basset JY. Diagnosis of cerebral metastasis by thallium-201. *Br Radiol* 1980;53:443-453.
 21. Van der wall Hans, Murray IPC, Huckstep RL, Philips RL. The role of scintigraphy in excluding malignancy in bone. *Clin Nucl Med* 1993;18:551-557.
 22. Tennvall J, Palmer J, Cederquist E, et al. Scintigraphic evaluation and dynamic studies with thallium-201 in thyroid lesions with suspected cancer. *Eur J Nucl Med* 1981;6:295-300.
 23. Yui N, Kinoshita F, Shimada F. Clinical evaluation of head and neck tumor scintigram with ^{201}Tl -chloride. *Kaku Igaku* 1979;16:221-227.
 24. Sehweil AM, Mckillop JH, Milroy R, et al. Thallium-201 scintigraphy in the staging of lung cancer, breast cancer and lymphoma. *Nucl Med Commun* 1990;11:263-269.
 25. Britten JS, Blank M. Thallium activation of the (Na^+ - K^+) activated ATP-ase of the rabbit kidney. *Biochem Biophys Acta* 1968;159:160-166.
 26. Sehweil AM, Mckillop JH, Milroy R, Wilson R, Abdel-Dayem HM, Omar YT. Mechanism of Tl-201 uptake in tumors. *Eur J Nucl Med* 1989;15:376-379.

Scatter

(Continued from page 3A)

radiation safety officers nod approvingly to committees assembled to develop policy for this practice. I have met oncologists who will not schedule patients for an office visit on the day of a bone scan because they are anxious about their own exposure to the radiation from the patient.

Although I do not argue with prudent radiation safety procedures, regulatory agencies and radiation safety personnel have fostered the erroneous notion that all detectable radiation is dangerous, that regulatory limits indicate dangerous levels of exposures and that risks exist at all levels of exposure. This evolves into the notion that all detectable radiation is dangerous and represents meaningful risk and that some cancers are caused by any exposure above background. No mention is made that background levels may vary in magnitude in various locales and that the incremental background exposure in certain areas is many times the exposure received from certain occupational activities. Despite intense scrutiny of these high background areas for many years, no adverse effect on the population has been observed.

I wonder what the Martians think of all this?

Stanley J. Goldsmith, MD

Editor-in-Chief, The Journal of Nuclear Medicine

October 1995